ACHIEVING DESIRED MODAL DAMPING RATIOS IN LUMPED SEGMENT CONTINUOUS SYSTEM MODELS

D. Geoff Rideout
Dept. of Mechanical Engineering, Memorial University, St. John's, NL, A1B 3X5, Canada,
g.rideout@mun.ca

ABSTRACT

For continuous systems, lumped segment models may be easer to generate than modal expansion models, especially when for varying cross-section geometry or material properties. However, there is no analytical correspondence between segment damping coefficients and modal damping ratios. Lumped segment modeling of a system with experimentally-determined damping ratios presents a resistive element tuning challenge. This paper treats R-element tuning as an optimization problem. Design variables include the coefficients of the familiar R-elements that are in parallel with bending, torsional, or axial compliance elements; along with additional R-elements that act on the absolute flow of the segment inertias. At each optimization step, damping ratios are determined from the current state variable coefficient matrix, which is a function of the resistances. For axially-vibrating rod and beam bending case studies, the first four desired modal damping ratios were achieved using the lumped segment R-element values from a fast-converging sequential quadratic programming optimization run.

Keywords: lumped segment, damping, optimization, modal damping ratio

1 INTRODUCTION

For modeling continuous systems such as rods, beams, or shafts, both the lumped-segment or modal-expansion methods readily lend themselves to bond graph implementation. While the modal expansion method can be more computationally efficient, as only N modes are required to capture the first N natural frequencies; the determination of mode shapes and natural frequencies can be analytically intractable. For the author's research on non-destructive evaluation of wooden structures using modal impact testing, models of tapered in-ground poles are required. Damping ratios from these models must match experimentally-measured values. While the lumped-segment method allows for straightforward inclusion of the varying cross section and compliant boundary conditions, the replication of modal damping ratios presents an R-element tuning challenge (Rideout and Whelan 2014). There is no analytical relation between modal damping ratios and the resistances of the typical R-elements that are placed in parallel with axial, torsional, shear, or bending compliances to account for material damping. The difficulty of modeling damping from first principles is acknowledged in (Karnopp, Margolis and Rosenberg 2012), wherein the tuning of damping ratios in modal expansion models is straightforward and gives accurate results. The tuning of lumped segment damping to achieve comparable modal damping ratios remains unresolved. A sample of the literature suggests that the typical approach to modeling damped beams is to add damping terms to the partial differential equation and solve using approximate or energy methods (Mahapatra and Panigrahi 2019), (Akinpelu 2012), as opposed to adding and tuning damping in a lumped segment model.

In this paper, lumped segment damping values are tuned through an optimization problem in which the symbolic coefficient matrix ("A" matrix) is generated, containing variables for the typical R elements in parallel with compliances, and additional "absolute" R elements that act directly on the inertial velocities. The damping ratios are

ICBGM'2021 Nov 8-10, 2021- San Diego, California USA - ©2021 Society for Modeling & Simulation International (SCS)

extracted from the *A* matrix eigenvalues at each optimization step and compared to the desired values, after which another optimization step is executed until convergence. Section 2 considers an axially vibrating rod for which the *A* matrix is generated by hand, and is scalable to an arbitrary number of segments. The segment bond graph submodel is reviewed, the Matlab generation of the *n*-dimensional *A* matrix and subsequent optimization problem are presented, and the dampers are tuned for multiple sets of desired modal damping ratio values. Section 3 applies the method to a more complex beam bending example, where the symbolic *A* matrix is generated using the Frequency Domain Toolbox of the 20sim® bond graph simulation environment. Section 4 discusses the results, and Section 5 provides a summary and description of future work.

2 DAMPER TUNING METHOD APPLIED TO AXIALLY VIBRATING ROD

2.1 Axial Vibration Model

The axially-vibrating rod is represented by a conceptually simple lumped segment model, with system schematic and segment submodel shown in Figure 1.

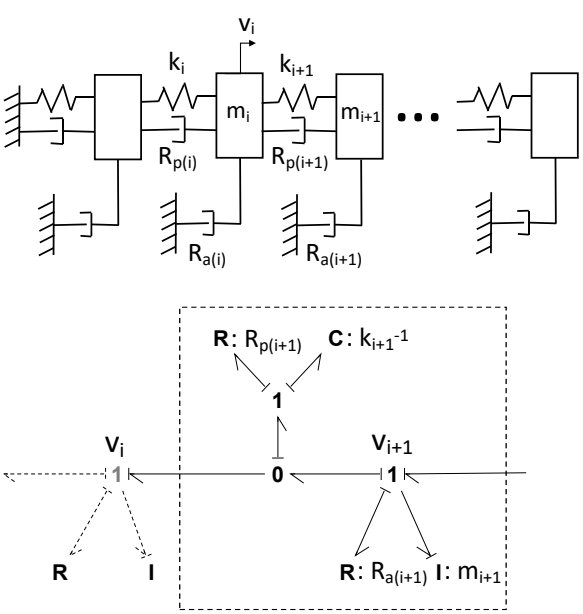

Figure 1: Axial vibration schematic and segment bond graph.

While the "absolute" dampers are more difficult to associate with physical phenomena that significantly affect the response, they will be shown to be useful for tuning modal damping ratios.

2.2 Simulation and Optimization

Based on a free body diagram of an individual segment, the *2n* x *2n* state coefficient matrix *A* for an *n*-segment representation can be expressed symbolically as in Table 1, assuming a state vector of the form $\dot{\vec{x}} = [x_1 \quad v_1 \quad x_2 \quad v_2 \ldots]$ where $\dot{x}_i = v_i$.

Table 1: Symbolic A matrix entries.

Element(s)	**Symbolic Expression**
Row *2i - 1*	Element *2i-1* = 1, all others 0
Row *2i*, element *2i*	$-\frac{R_{pi} + R_{p(i+1)} + R_{ai}}{m_i}$
Row *2i*, element *2i-1*	$-\frac{k_i + k_{(i+1)}}{m_i}$
Row *2i*, element *2i+1*	$\frac{k_{(i+1)}}{m_i}$
Row *2i*, element *2i+2*	$\frac{R_{p(i+1)}}{m_i}$
Row *2i*, element *2i-2*	$\frac{R_{p(i+1)}}{m_i}$
Row *2i*, element *2i-3*	$\frac{k_i}{m_i}$

The expressions in Table 1 were coded into a Matlab® m-file, using symbolic variables for mass, stiffness, and damping coefficients. Because the *A* matrix variable remains symbolic even after substituting constant parameter values for mass and stiffness, the *A* matrix was copied and pasted into a function m-file as a double-precision variable. The "Rp_" and "Ra_" variable names appear in the *A* matrix, and must be defined in the preceding code as the elements of the function argument vector. At each optimization step, the current values of the damping coefficients are passed to this function and substituted into the *A* matrix. Eigenvalues are calculated and sorted by increasing mode number, and then damping ratios

Z_i, are computed and compared to the desired (reference) damping ratios Z_{ir} according to a weighted cost function. Figure 2 shows excerpts of the Matlab code, and Equation (1) is the cost function.

$$J = \sum_i a_i \left(Z_i - Z_{ir}\right)^2 \qquad (1)$$

```
function J = DampMatch_ap(X)
% Compute eigenvalues and damping
% ratios for current values of R
%
% Desired damping ratios
global Z1r Z2r Z3r Z4r a;

% Redefine X elements
Ra1 = X(1);  % Ra are "absolute" dampers
Ra2 = X(2);
.
.
Rp17 = X(35); % Rp are "parallel" dampers
Rp18 = X(36);

A =   [0 1 0 . . . . .
      -8244 -0.229*Ra1-0.229*Rp1-0.229*Rp2 . .


% Determine eigenvalues and
% sort by magnitude
EAS = sortrows(eig(A));
[Wn,Z] = damp(EAS); % Compute damping ratios
% Extract first four desired damping ratios
% (two are calculated for each mode)
ZR = [Z(1) Z(3) Z(5) Z(7)]
```

Figure 2: Damping ratio calculation in Matlab®

2.3 Results

Figures 3-6 depict the first four mode shapes of the bar, while also plotting parallel damping values vs. axial coordinate (orange long-dash line), and absolute damping values vs. axial coordinate (blue solid line). The absolute damping values are scaled so that the variation along the bar length is clear. The plot titles show the desired and tuned damping ratios in percent. Bar properties, based on a fictitious material that exaggerates displacements without impacting the generality of the method, are: Young's modulus 100 x 10^3 Pa, density 7860 kg/m^3, cross-sectional area 0.01 m^2, length 1 m.

From the figure titles it is apparent that the desired damping ratios can be achieved with reasonable accuracy, given that there is a five-fold increase of one of the ratios. The coefficients of the absolute dampers, which act directly on the velocity of each mass, are typically 1-2 orders of magnitude lower than those for the parallel dampers, for a given amount of overall damping. The parallel dampers act on the relative velocity of adjacent segments, which is much smaller than the absolute velocity.

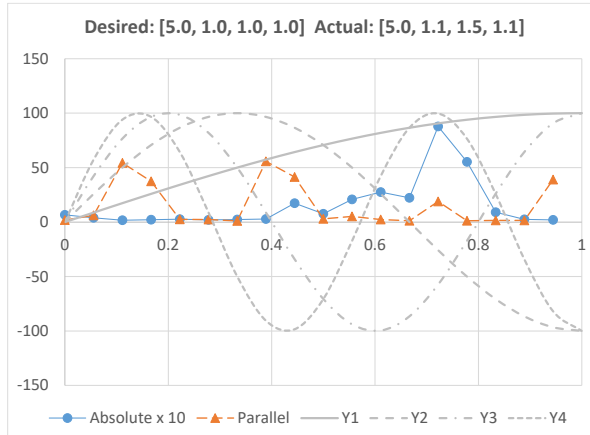

Figure 3: Z_{ir} = [5%, 1%, 1% 1%]

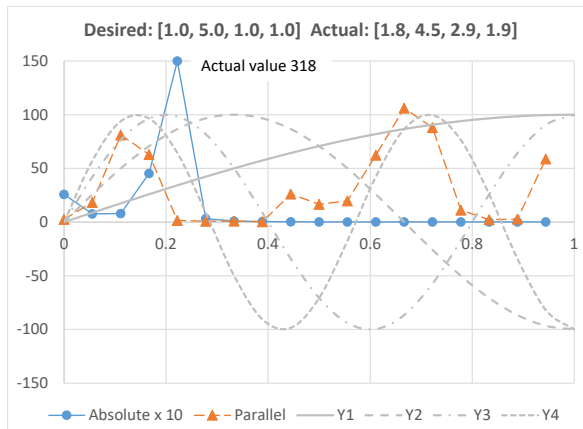

Figure 4: Z_{ir} = [1%, 5%, 1% 1%]

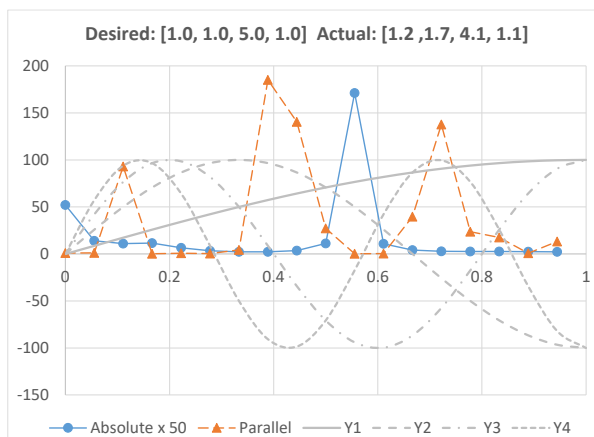

Figure 5: Z_{ir} = [1%, 1%, 5% 1%]

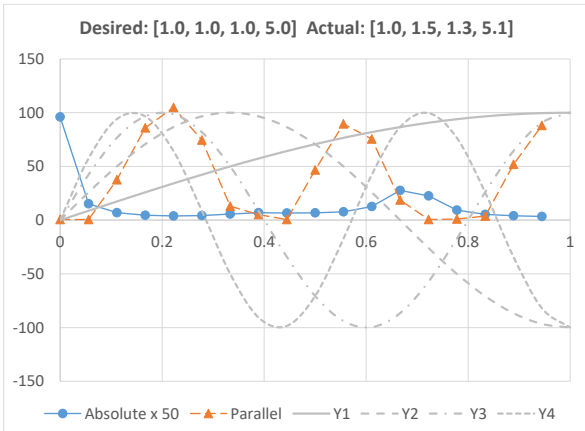

Figure 6: Z_{ir} = [1%, 1%, 1% 5%]

Figure 7 shows the response of the bar with only absolute dampers (R_a = 1 Ns/m), and then with only parallel dampers (R_p = 150 Ns/m), with each model giving the same first damping ratio. Table 2 shows the associated natural frequencies and damping ratios. For parallel dampers, damping ratios increase monotonically, while for absolute dampers they decrease. The response at the peaks in Figure 7 therefore shows more persistent high-frequency content for the case of absolute damping only. A combination of absolute and parallel damping is required for arbitrary ratio tuning.

Table 2: Damping ratios, equal R values.

	Absolute Dampers Only (R_a = 1 Ns/m)	**Parallel Dampers Only (R_p = 150 Ns/m)**
Nat'l Freq (rad/s)	**Damping Ratio (%)**	**Damping Ratio (%)**
5.45	2.1	2.3
16.31	0.70	6.8
27.05	0.42	11.3
37.6	0.30	15.7

The locations of the elevated damping coefficients with respect to the modal nodes and antinodes is addressed in the Discussion section.

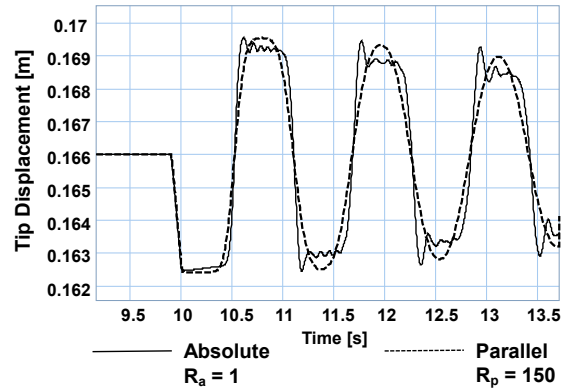

Figure 7 – Time response comparison.

3 EXTENSION TO BEAM BENDING WITH COMPUTER-GENERATED *A* MATRIX

3.1 Methodology

The optimization method is now applied to the more complex beam bending model. A 20-segment Euler-Bernoulli beam model was constructed with absolute dampers acting on the lateral translational segment velocity, and parallel dampers acting on the rotational (bending) relative velocity of adjacent segments. The schematic and segment bond graph are shown in Figure 8.

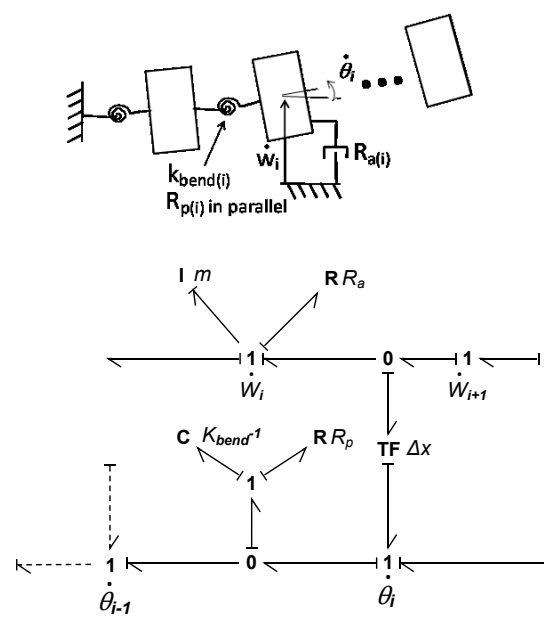

Figure 8: Euler-Bernoulli beam schematic and segment bond graph

The increase in complexity compared to the axially-vibrating rod necessitated the use of the 20sim® Frequency Domain Toolbox to generate a symbolic A matrix. As shown in the Figure 9 screen shot, the symbolic A matrix is cumbersome, but can be exported to Matlab® as an m-file script. The constant parameters (e.g., length L, Young's Modulus E) were substituted, the variable names simplified, and the matrix pasted into a function m-file as in the Section 2 example. As a test, the function was used to predict the system eigenvalues, which matched the 20sim® eigenvalues from a numeric linearization based on the time response to an impulse force as shown in Figure 10. In this numerical test case, all absolute and parallel damper values were set to 1.0. Beam properties: Young's modulus 8.47 GPa, density 320 kg/m^3, cross section 0.0889 m x 0.0889 m, length 1.0668 m.

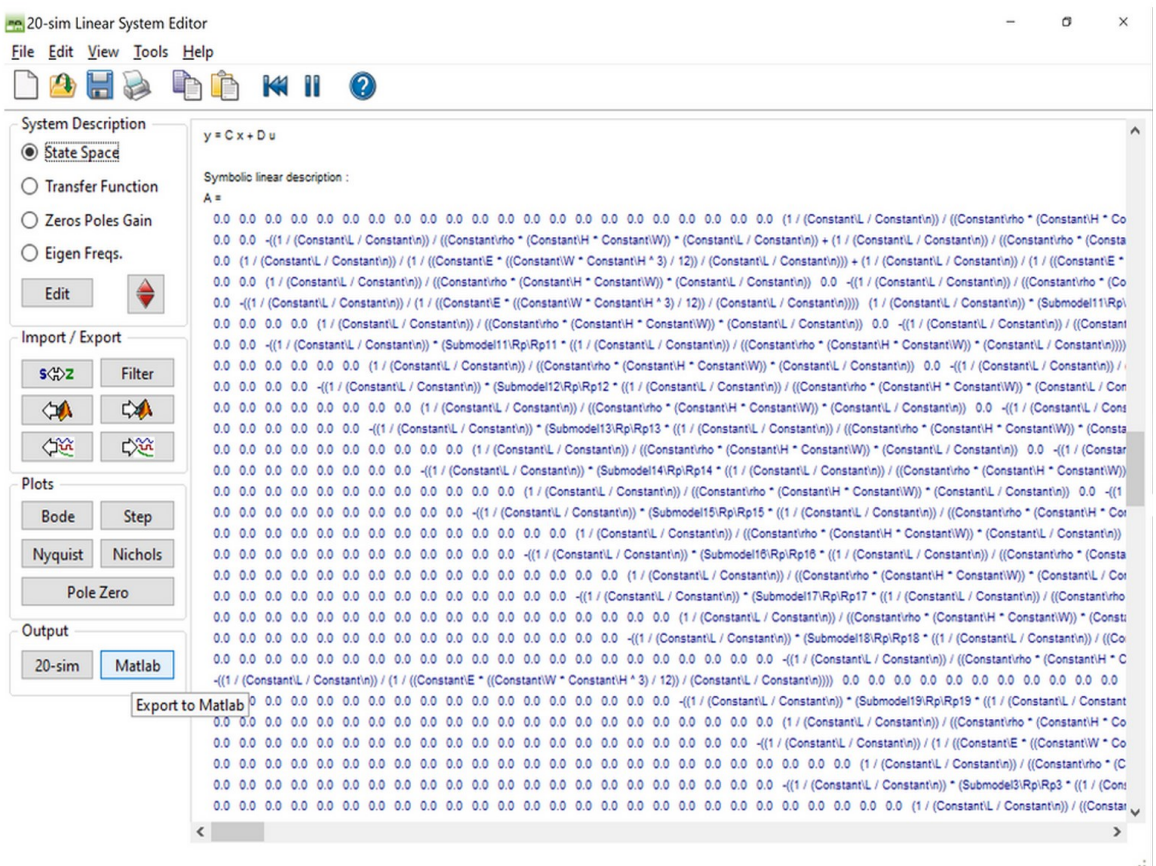

Figure 9: Portion of symbolic A matrix from 20sim®

Upon reinstating the damper coefficients as optimization design variables, the tuning problem was solved as in Section 2. The method worked without issues for the even more complex problem of the Timoshenko beam with rotary damping and translational shear (resulting in an 80 x 80 A matrix); however, only the Euler-Bernoulli results are shown in this paper.

3.2 Results

Table 3 shows the weighting factors, target, and actual damping ratios for the Euler-Bernoulli beam, using the same four sets of desired values as in the axial case study. Default settings were used for Matlab®'s *fmincon* optimization command except that maximum iterations were increased to 5000 from 3000. Despite increasing the weighting factor of the mode 2 damping ratio in the second scenario of Table 3, the first damping ratio could not be suppressed fully. Interactions among damping ratios are complex, and there appear to be limits on how greatly successive damping ratios can vary relative to each other. The first mode has no node other than the fixed end, and any attempt to add damping to mode 2 must affects mode 1. This issue is discussed further in Section 4.

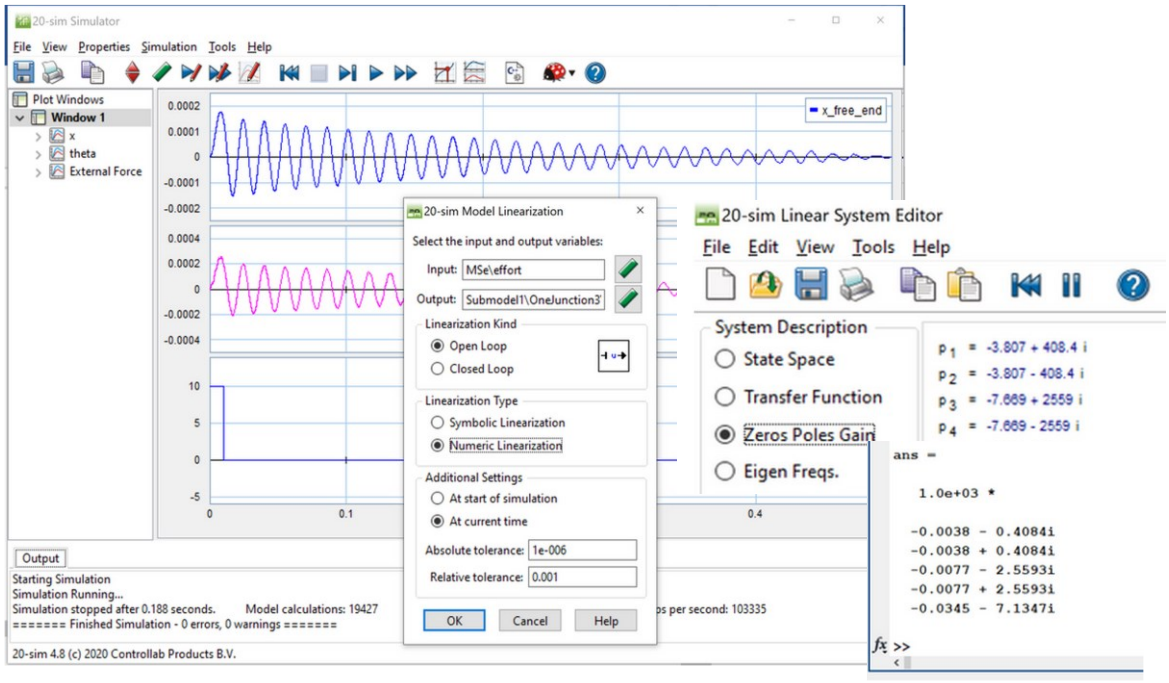

Figure 10: Time response and eigenvalue verification.

Table 3 – Bending beam damping ratio tuning results.

Desired Damping Ratios (%)	**Weighting Factors**	**Final Damping Ratios (%)**	**Objective Function Final Value**
5, 1, 1, 1	1000, 1000, 1000, 1000	5.0, 1.0, 1.0, 1.0	5.5465e-10, converged within tolerances
1, 5, 1, 1	1000, 10000, 1000, 5000	3.3, 4.8, 1.9, 1.2	0.6638, maximum iterations exceeded
1, 1, 5, 1	1000, 1000, 1000, 1000	1.0, 1.4, 4.9, 1.1	0.0149, maximum iterations exceeded
1, 1, 1, 5	1000, 1000, 1000, 1000	1.0, 1.0, 1.0, 5.0	3.4967e-09, converged within tolerances

Figure 11 shows time response for both a modal expansion model and a tuned lumped segment model with desired modal damping ratios of [1%, 1%, 5%, 1%]. The two models show excellent agreement, verifying that the tuning results lead to the anticipated modal damping ratios in the bond graph.

4 DISCUSSION

Early investigations with the 18-segment axial rod showed that completely arbitrary damping ratios could not be realized, given that individual damping values for one segment will affect other modal damping ratios. An attempt to achieve three widely-varying ratios Z_{ir} = [12%, 2%, 12%] resulted in a best result of [12.9% 2.4% 8.6%] based on trial and error initial conditions and weighting factors. There are limits to how much the second mode damping can be suppressed for the bar, if the third mode must then be raised to a significantly higher value. Section 3 showed that raising mode 2 damping without raising that of mode 1 was not achievable for the beam.

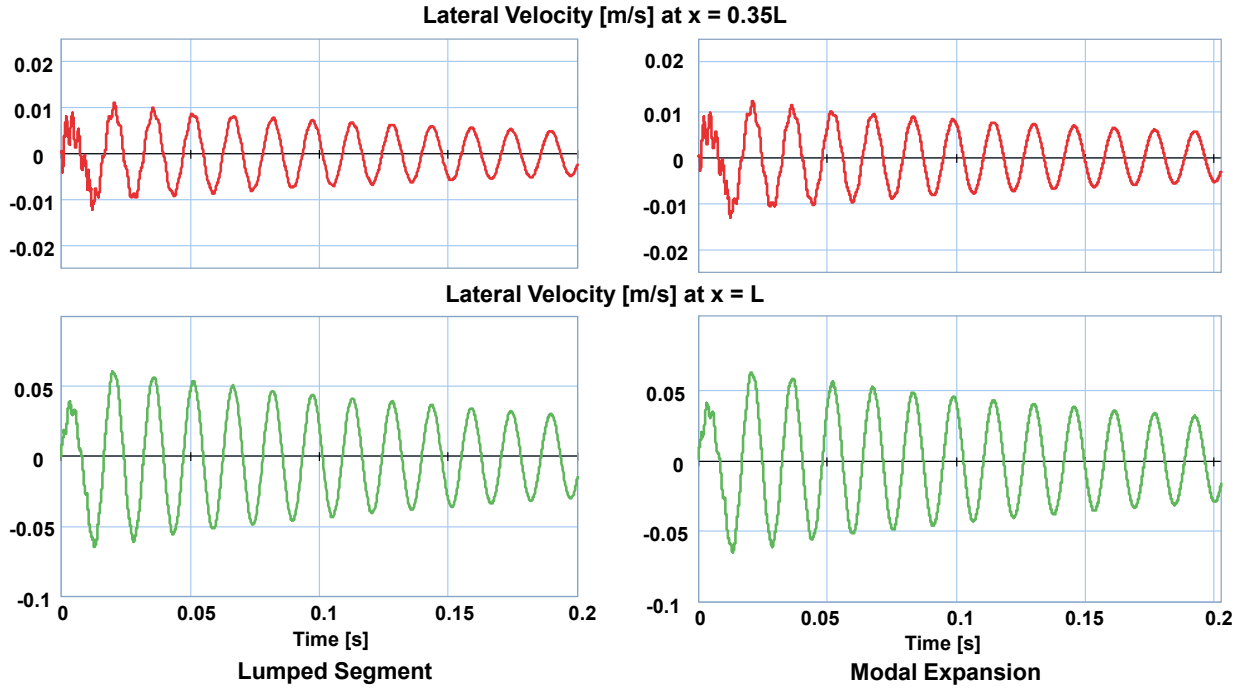

Figure 11: Time response of lumped segment and modal expansion beams with Z_{ir} = [1%, 1%, 5% 1%].

For the [1.0% 1.0% 1.0% 5.0%] bar tuning problem, an *ad hoc* method of raising the damping of mode 4 was attempted by putting high damping only at the antinodes of mode 4. This did increase mode 4 damping but also increased damping of mode 1. The tuning problem is more complex than simply inserting or removing dampers at locations of modal nodes and antinodes. For example, Figure 3 shows elevated parallel damping at all antinodes of mode 4, and elevated absolute damping at the third antinode of mode 4; yet only mode 1 damping ratio is elevated. Figure 4 is somewhat more intuitive in that mode 2 damping ratio must be raised, and as expected, little parallel damping is present at the first antinode of mode 2. However, extremely high absolute damping is placed at a segment that should contribute significantly to modes 2, 3, and 4. Figure 5 shows elevated parallel damping near two of the three *nodes* of mode 3, yet mode 3's damping ratio is elevated (likely via the higher absolute damping at the second antinode). Given that there is overlap of nodes and antinodes for various modes, the tuning problem is necessarily not easily predicted or derived.

5 SUMMARY AND FUTURE WORK

For modeling applications where the simplicity of a lumped-segment bond graph modeling approach is warranted (e.g., varying cross-section), yet particular modal damping ratios are required (e.g., to match experimental modal testing results), the damper tuning problem has been solved using optimization. Both "parallel" dampers (in parallel with material compliances) and "absolute" dampers (responding to inertia velocities) were treated as optimization design variables in a Matlab® fmincon sequential quadratic gradient search method. The optimizer calculated damping ratios at each step based on a state coefficient matrix that was generated by hand for an 18-segment axially-vibrating rod, and using 20sim®'s Frequency Domain Toolbox for a 20-segment Euler-Bernoulli beam in bending.

Future work could include using a Monte Carlo simulation to vary weighting factors and initial conditions in search of global optima. In the beam bending case study, damping could also have been added to the absolute angular rotation (bending) 1-junctions. Nonlinear damping laws could also be considered in search of greater capacity to achieve damping ratios which vary considerably from one mode to the next.

ACKNOWLEDGMENTS

The author would like to acknowledge Mateo Vergara, an inquisitive and talented undergraduate student who stumbled upon an atypical pattern of modal damping ratios while working on a lumped segment model for a course assignment. The idea for this paper came from that discovery.

REFERENCES

Rideout, D. G., and O. F. Whelan. 2014. "Modeling of Tapered Cantilever Beams for Simulation of Utility Pole Vibration". In *Proc. International Conference on Bond Graph Modeling and Simulation ICBGM'14*, edited by J. J. Granda and D. C. Karnopp. San Diego, California, Society for Modeling and Simulation International.

Karnopp, D. C., D. L. Margolis, and R. R. Rosenberg. 2012. *System Dynamics: Modeling, Simulation, and Control of Mechatronic Systems* (5 ed.). Hoboken, New Jersey, John Wiley and Sons.

Mahapatra, K. and S. K. Panigrahi. 2019. "Dynamic Response of a Damped Euler–Bernoulli Beam Having Elastically Restrained Boundary Supports". *J. Inst. Eng. India Ser. C* vol. 6, pp. 891–905.

Akinpelu, F. O. 2012. "The Response of Viscously Damped Euler-Bernoulli Beam to Uniform Partially Distributed Moving Loads". *Applied Mathematics* vol. 3, pp. 199-204.

AUTHOR BIOGRAPHIES

D. GEOFF RIDEOUT is a Professor of Mechanical Engineering at Memorial University in St. John's, Newfoundland, Canada, where he earned his Bachelor's Degree. He has an M.A.Sc.(Eng.) from Queen's University in Canada, and a Ph.D. from the University of Michigan Ann Arbor. His current research interests are vehicle dynamics, simulation-based design of oil well drill strings, and vibration-based non-destructive testing of electrical utility poles. He is a registered professional engineer in Newfoundland. His email address is g.rideout@mun.ca.